JOURNAL OF GAS TECHNOLOGY

Volume 5 / Issue 1 / Summer 2020 / Pages 42-51

Journal Homepage: http://jgt.irangi.org

Intensification of liquid fuel production using Nano Fe Catalyst in GTL process

Mohammad Irani[1*], Asghar Alizadehdakhel[2] , Yahya Zamani[1]

1. Research Institute of Petroleum Industry (RIPI), Tehran, Iran
2. Rasht Branch, Islamic Azad, Rasht, Iran

ARTICLE INFO

ORIGINAL RESEARCH ARTICLE

Article History:
Received: 24 April 2020
Revised: 23 June 2020
Accepted: 11 August 2020

Keywords:
Fischer-Tropsch Synthesis
GTL
Fixed bed reactor
Nano Fe Catalyst
CFD

ABSTRACT

An experimental and computational fluid dynamic (CFD) investigation was carried out to intensify the production of gasoline in a bench-scale Fischer-Tropsch Synthesis (FTS) process. A cylindrical reactor with one preheating and one reaction zone was employed. The reactor temperature was controlled using a heat jacket around the reactor's wall and dilution of the catalyst in the entrance of the reaction zone. An axi-symmetric CFD model was developed and the non-ideality of the gas mixture was considered using Peng-Robinson equation of state. A kinetic model based on 25 chemical species and 23 reactions was utilized. The model validated against experimental measurements and the validated model employed to investigate the effects of operating conditions on the performance of the reactor. The optimum values of operating conditions including pressure, reactor temperature, GHSV and H_2/CO ratio were determined for maximum reactor performance.

DOR: 20.1001.1.25885596.2020.5.1.4.4

How to cite this article
M. Irani, A. Alizadehdakhel, Y. Zamani. Intensification of liquid fuel production using Nano Fe Catalyst in GTL process. Journal of Gas Technology. 2020; 5(1): 42 -51. (http://www.jgt.irangi.org/article_251659.html)

*Corresponding author.
E-mail address: iranim@ripi.ir (M. Irani)

Available online 20 September 2020

1. Introduction

The conversion of syngas (CO + H_2 mixtures) into liquid fuels via Fischer-Tropsch synthesis (FTS) has attracted much attention in the recent years. The increase in global energy demand, existence of numerous gas reservoirs in remote areas and the high price of crude oil in comparison with natural gas, are the main reasons of the increasing attention to FTS. In addition, converting of associated gases is appealing due to economic and environmental reasons. Also, GTL products are almost free of sulfur and aromatic hydrocarbons. Composition of the obtained products depends on the employed catalysts and operating conditions [1,2]. Numerous researches have been carried out to understand, model and optimize this process. Butt et al. [3] prepared and characterized Fe and Fe-Co catalysts on ZSM-5 support for FTS. Schulz et al [4] investigated the selective conversion of syngas to gasoline on iron/HZSM5 catalysts. The effects of temperature, space velocity, CO/H_2 feed ratio and pressure on the activity of a Co/HZSM5 zeolite bifunctional catalyst were experimentally investigated by Calleja et al [5]. The fixed-bed FT process, is one of the most competing reactor technologies and occupies a special position in FTS industrial processes [6]. Liu et al [7] developed a two-dimensional heterogeneous model for simulation of steady and unsteady behavior of a fixed bed FTS reactor. They also reported [8] the effects of feed temperature, flow rate and wall temperature on the steady state behavior of the reactor. Wang et al [9] developed a one-dimensional heterogeneous model to predict the performance of fixed-bed Fischer-Tropsch reactors. Rahimpour et al [10] proposed a novel combination of fixed-bed and slurry bubble column membrane reactor for Fischer-Tropsch synthesis. In the first catalyst bed, the synthesis gas was partially converted to hydrocarbons in a water-cooled fixed bed reactor. In the second bed which was a membrane assisted slurry bubble column reactor, the heat of reaction was used to preheat the feed synthesis gas to the first reactor. The membrane concept was suggested to control hydrogen addition. They utilized a one-dimensional packed-bed model for simulation of fixed-bed reactor. A one-dimensional model with plug flow pattern for gas phase and an axial dispersion pattern for liquid-solid suspension was used for modeling of slurry bubble column reactor. They claimed that their proposed reactor system gives favorable temperature profile and higher, gasoline yield, H_2 and CO conversion as well as selectivity. However, they admitted that experimental proof of concept is needed to establish the validity and safe operation of the proposed reactor. Nakhaei Pour et al [11] developed a kinetic model for water-gas-shift (WGS) reaction over a Fe/Cu/La/Si catalyst under Fischer-Tropsch synthesis (FTS) reaction condition. By comparing the results of four different models over a wide range of reaction conditions, they found that WGS rate expressions based on the format mechanism best fit the experimental data. Although the reaction scheme has been studied and used for a long time, its study today is still of interest because of the high pressure on hydrocarbons prices all over the planet. In the recent years, by the high speed of computational calculations, Computational Fluid Dynamics (CFD) techniques have become a useful tool for simulation and analysis of variety of industrial problems that deal with fluid flow [12-14], heat and mass transfer [15,16] and chemical reactions[17, 18]. By predicting a system's performance in various conditions, CFD can potentially be used to improve the efficiency of existing units as well as the design of new systems. It can help to shorten product and process development cycles, optimize processes in order to improve energy efficiency and environmental performance, and solve problems as they arise in plant operations. However, it is essential to validate the CFD results against data obtained from real operating systems. Krishna and Van Baten [19 and 20] employed CFD technique for describing hydrodynamics of bubble column reactors and its effects on scaling up this type

of reactors. Jiang et al [21] used a CFD approach for obtaining the detailed flow field and bubble behaviors in a novel two-stage fluidized bed reactor which was designed to produce diethyl oxalate from carbon monoxide based on the catalytic coupling reaction. A FTS microchannel reactor was modeled in three-dimensions by Arzamendi et al [22]. They utilize a CFD model to analyze the effects of feed and cooling water flow rates and pressure on the performance of the reactor. In our previous work, FTS fixed bed reactor based on Iron-zeolite catalyst was studied and the use of saturated water for absorbing the heat of reaction was investigated. It was concluded that the temperature run away was controlled by utilizing saturated water, and the maximum temperature rising within the catalyst bed was 16K [23]. In the present work, a CFD model was developed to model FTS in a fixed bed nano-iron catalyst reactor. The catalyst bed was diluted in the entrance region of the bed in order to prevent hot spots. Thermodynamics properties of the gas mixture were calculated using Peng-Robinson equation of state [24]. The model predictions were validated with measured data and the effect of operating conditions on performance of the reactor were analyzed.

2. Material and Methods

2.1. Process description

The employed reactor was a 1.2 cm diameter cylindrical reactor which was placed inside a heating jacket (Figure 1). The reactor included a preheating zone with 30cm height following by a reaction zone with 50cm height. It was designed and constructed by the Research Institute of Petroleum Industry, National Iranian Oil Company (RIPI-NIOC) in 2010 [25]. The reactor was packed with cylindrical Fe-Sio2 catalysts (atomic ratios: 100Fe/5.64Cu/2La/19Si) with average diameter and length of 0.3 mm and 0.9 mm, respectively. Particle and bulk densities of the catalyst were 1290 and 730 kg/m^3, respectively. Entrance region of the reaction section was diluted using ceramic particles in order to prevent the creation of hot spot.

Figure 1. FTS fixed-bed reactor used for experiments

The experiments were run at different conditions of feed temperature, pressure, GHSV and H_2/CO ratio as given in table 1.a

Table1. Operating conditions

Feed Temperature(K)	543,563, 583 and 603
Reactor pressure(bar)	13,17,21 and 25
GHSV(hr $^{-1}$)	1800, 5500,11000 and 15000
H_2/CO molar ratio	0.5, 1,1.5 and 2

2.2. CFD Modeling

2.2.1. Geometry and solution strategy

The reactor was modeled using a 1.2 cm × 80 cm axi-symmetric model. The computational domain was divided into 22,016 rectangular meshes and the predicted profiles of temperature and species mole fractions were checked to be independent of the mesh size. The packed bed was considered as a porous

media due to the large value of tube to catalyst diameter ratio (N>12) [26].

The entrance region of the reaction zone was considered as diluted reaction zone and the reaction rates in this zone were multiplied by catalyst/ (catalyst + ceramic) ratio. Mass-flow-inlet and pressure-outlet boundary conditions were used for reactor inlet and outlet, respectively. Constant temperature and no-slip conditions were employed for the reactor walls. The finite volume method was used to discretize the partial differential equations of the model. The SIMPLE algorithm was employed for pressure-velocity coupling. The convergence criterion was based on the residual value of the calculated variables, namely mass, velocity components, energy and species mass fractions. In the present calculations, the numerical computation was considered to be converged when the scaled residuals of the different variables were lower than 10^{-4} for continuity and momentum equations and 10^{-7} for the other variables.

2.2.2. Conservation equations

The mass conservation, momentum, energy and species, can be expressed as:

Mass: $\nabla.(\vec{v}\rho\ ) = 0$ (1)

Momentum: $\nabla.(\rho\vec{v}\vec{v}) = -\nabla P + \nabla.\left[\mu\left(\nabla\vec{v} + \nabla\vec{v}^{T}\right)\right] + \rho g + S$ (2)

Energy: $\nabla.(\vec{v}(\rho\ H\ + P)) + \nabla.(\sum_{i=1}^{n} h_i j_i) = -\nabla.(q) + S_R$ (3)

Species: $\nabla.(\vec{v}C_i - D_i\nabla C_i) = R_i$ (4)

Where, ρ represents mixture density, $\vec{v}$ is velocity vector, H and hi are total enthalpy and enthalpy of species, respectively. P is the static pressure and C_i stands for concentration of chemical species. The porous media of the reaction zone was modeled by addition of a momentum source term:

$$S = -\left(\sum_{j=1}^{2} D_{ij}\mu v_j + \sum_{j=1}^{2} C_{ij}\frac{1}{2}\rho|v|v_j\right) \quad (5)$$

The first term on the right-hand side of equation 5 is the viscous loss term and the second term is the inertial loss term. $|v|$ is the magnitude of the velocity and D and C are prescribed matrices. In this work, flow in the reactor is laminar; therefore, the inertial term was ignored [27]. (FLUENT 6 User manual). S_R in equation (3) is the source of energy due to chemical reaction:

$$S_R = -\left(\sum_j \frac{h_j^0}{M_j} R_j\right) \quad (6)$$

2.2.3. Physical properties

Peng-Robinson equation of state was used to predict the non-ideality [16]of the gas mixture:

$$\ln\tilde{\varphi}_i = (Z-1)\frac{b_i}{b_m} - \ln(Z-beta) - I\bar{q}_i \ ,\ q = \frac{a}{bRT} \ ,\ \bar{q}_i = q\left(2.\times\frac{\frac{\partial a}{\partial x_i}}{a} - \frac{b_i[i]}{b}\right)$$

$$I = \frac{1}{\varepsilon_1 - \varepsilon_2}\ln\left(\frac{Z+\varepsilon_1\times beta}{Z+\varepsilon_2\times beta}\right) \ ,\ beta = \frac{bP}{RT} \ ,\ f_i = \tilde{\varphi}_i\times P\times y_i \quad (7)$$

Where, f_i is species fugacity, R is the universal gas constant, MG is the molecular weight of gas mixture and P is the operating pressure (taken to be 17 bar). Z is the compressibility factor for calculation of the mixture density:

$$\rho = \frac{PM}{Z\,R\,T} \quad (8)$$

The parameters of equation (7) are listed in table 2. The specific heat of each species was defined as piecewise-polynomial function of temperature. Other thermal properties of the mixture such as molecular viscosity, thermal conductivity and diffusivity coefficient were calculated from Poling et al [28].

Table 2. Parameters of Peng-Robinson EOS

ε_1	ε_2	Ω	Ψ
$1+\sqrt{2}$	$1-\sqrt{2}$	0.07779	0.45724

$$Z^3-(1-B)Z^2+(A-2B-3B^2)Z-(AB-B^2-B^3)=0$$

$$A=\frac{aP}{(RT)^2}\ ,B=\frac{bP}{RT}$$

$$a=\sum_{i=1}^{n}\sum_{j=1}^{n}x_i x_j(a_i a_j)^{0.5}(1-k_{ij})\ ,\quad b=\sum_{i=1}^{n}x_i b_i$$

$$a_i=a_{ci}\alpha_i\ ,\ a_{ci}=\Psi\frac{(RT_{Ci})^2}{P_{Ci}}\ ,\ b_i=\Omega\frac{(RT_{Ci})}{P_{Ci}}$$

$$\alpha_i=\left[1+(0.37464+1.54226\omega-0.26992\omega^2)(1-T_r)^{0.5}\right]^2$$

2.2.4. Reaction rate expressions

The considered reactions with 25 chemical species including CO, H_2, CO_2, H_2O and C_1-C_{21} are listed in Table 3. The general form of rate equations [25] for production of C_i is expressed as:

$$R_{C_1}=.001518*f_{H2}^{\ 0.241}/f_{CO}^{0.241} \quad (10)$$

$$R_{C_2}=.01819*f_{H2}^{\ 0.045}/f_{CO}^{0.045} \quad (11)$$

$$R_{C_3}=0.025f_{H2}^{0.1}f_{CO}^{-0.8} \quad (12)$$

$$R_{C_i}=\frac{0.025f_{H2}^{0.1}f_{CO}^{-0.8}}{(2.03-0.14f_{H2}f_{CO}^{-1})^{i-1}}\quad i=4\text{-}9 \quad (13)$$

$$R_{C_{10}}=5e-5f_{H2}^{1.8}f_{CO}^{-1.1} \quad (14)$$

$$R_{C_i}=\frac{5e-5f_{H2}^{1.8}f_{CO}^{-1.1}}{(1.16-0.089f_{H2}f_{CO}^{-1})^{i-1}}\quad i=11\text{-}22 \quad (15)$$

Table 3. list of FTS reactions

Reaction Number	Reaction Stoichiometry
1-22	$nCO+(n+1)H_2\rightarrow C_nH_{2n+2}+nH_2O$, n = 1-22
23	$CO+H_2O\rightarrow CO_2+H_2$

Reaction (23) is known as water-gas-shift (WGS) reaction and its rate [11] can be expressed as:

$$R_{WGS}=\frac{k_w\left(f_{CO}f_{H2O}-f_{CO_2}f_{H2}/K_{WGS}\right)}{(1+K_1f_{CO}+K_2f_{H2O})^2} \quad (16)$$

The kinetic parameters of WGS reaction rate are given in table 4 where, K_{WGS} is the equilibrium constant and can be calculated as follows:

$$\log K_{WGS}=\left(\frac{2073}{T}-2.029\right) \quad (17)$$

Table 4. Rates parameters for WGS reaction

Parameter	Value
kw (mmol.grcat^{-1}.s^{-1}.bar^{-2})	0.77
k_1 (bar^{-1})	0.39
k_2 (bar^{-1})	3.54

3. Results and Discussion

Compressibility factor of the gas mixture is a criterion of its deviation from the ideal behavior. A contour plot of the predicted compressibility

factor along the reactor is shown in (Figure2). The figure shows that formation of heavy hydrocarbons causes the compressibility factor to descend to a value of about 0.9. Therefore, it is necessary to consider the mixture's non-ideality in calculation of density.

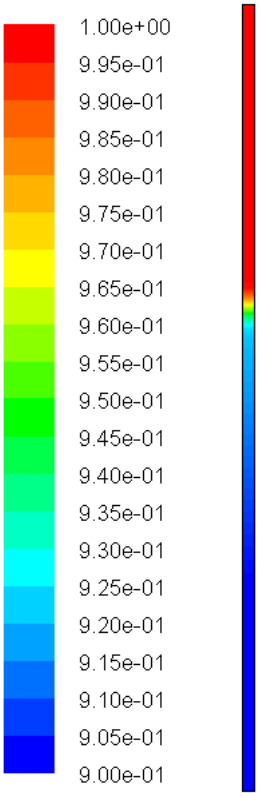

Figure 2. Gas mixture compressibility factor (Z) contour along the reactor
(T=573, P=17 bar, GHSV=5500 hr -1 and CO/H_2=1)

A comparison between the predicted and measured values of C_{5+} selectivity, CO conversion and temperature at three points (at the beginning, middle and end of the catalytic bed) along the reactor for two different operating conditions are given in table 5. The values in this table demonstrate that the error values are less than 4% for all of the compared variables. That is to say, the model in this work can successfully predict the performance of the fixed-bed FT process. Contour plots of temperature inside the reactor shown in (Figure 3) demonstrates that there is a temperature raise of about 17K in the beginning of the catalytic bed due to the high partial pressure of the reactants and the high rate of exothermic reactions in this region.

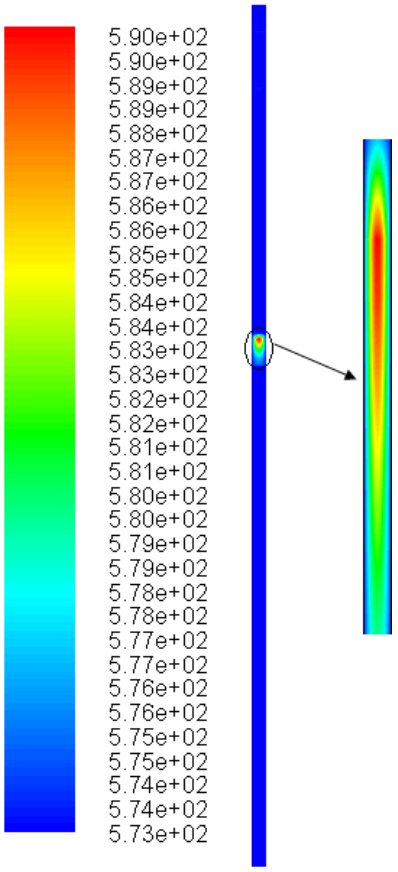

Figure 3. Contour of temperature
(T=573, P=17 bar, GHSV=5500 hr -1 and CO/H_2=1)

However, this amount of temperature raise is tolerable for this process and it could be claimed that the reactor was well controlled at the desired inlet temperature by dilution of the catalyst at the entrance of the reaction zone. Profiles of species mass fraction along the reactor are plotted in (Figure 4). Concentrations of the reactants (CO and H_2) are reduced due to their consumption along the reactor.

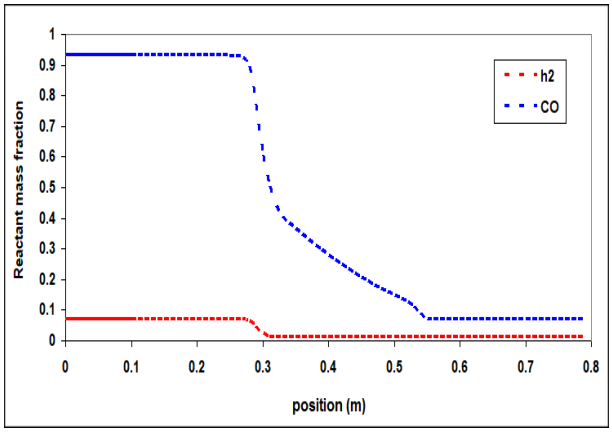

(a) Reactants

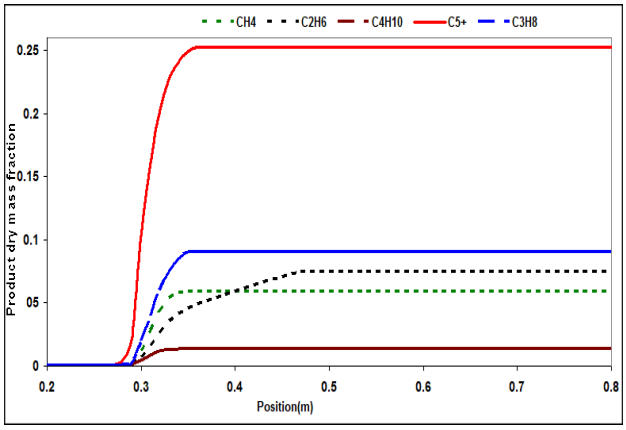

(b) Products

Figure 4. Mass fraction of species along the reactor length (T=573, p=17 bar, CO/H_2=1 and GHSV=5500 hr -1)

Therefore, the reaction rates are reduced and consequently the slopes of species concentration curves along the reactor are decreased. The figure shows that the main changes in the concentrations of reactants and products occur in the beginning of the catalytic zone except for CO and ethane. Ethane acts as a monomer or building block during the FTS. Readsorption of ethane will result in a decrease of the ethane yield and an increase of higher hydrocarbons [29 , 30]. This effect was included in ethane production rate (the power of CO and H_2 concentration in equation (11) is much less than that in other rate equations). The difference between the style of CO concentration profile and that of the other species can also be related to this effect. (Figure 5) interprets the mixture density along the reactor.

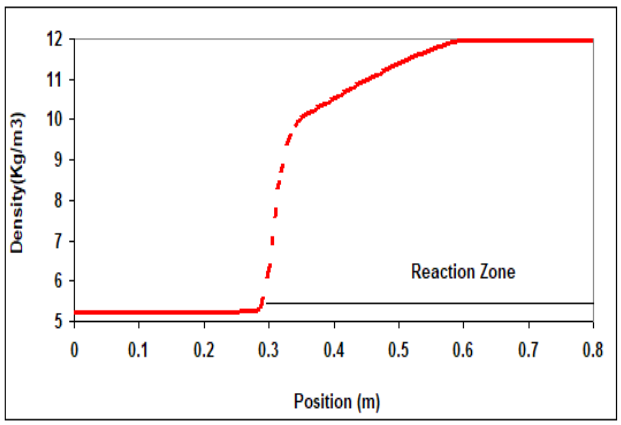

Figure 5. Profile of density
(T=573, P=17 bar, GHSV=5500 hr -1 and CO/H_2=1)

As expected, the mixture density increases along the reactor due to the formation of heavier hydrocarbons. The same reason can be used to describe the velocity reduction along the reactor as shown in (Figure 6). The parabolic radial velocity distribution (in the preheating zone) and zero velocity near the walls due to the no-slip wall boundary condition are also observed in this figure. In addition, pressure drop in the porous region causes the gas velocity to become almost uniform in the radial direction.

The reactor model was run at four different levels of each operating parameters (temperature, GHSV, pressure and H_2/CO ratio) and the effects of these parameters on the performance of the reactor were investigated. In all cases, one parameter was changed and the other parameters were kept constant.

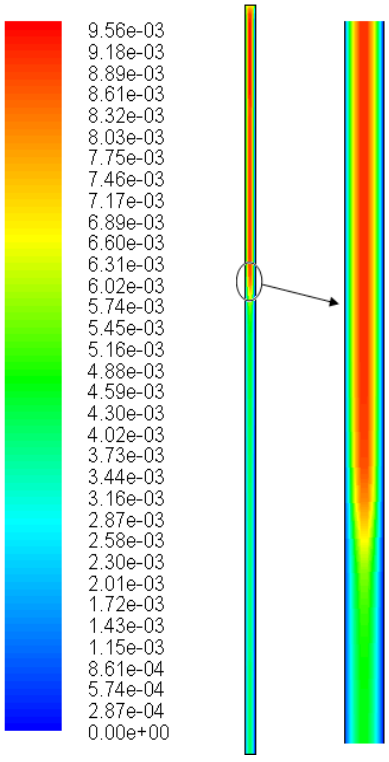

Figure 6. Contour of velocity
T=573, P=17 bar, GHSV=5500 hr -1 and CO/H_2= 1)

The effect of inlet temperature on C_{5+} selectivity (gr C_{5+}/gr converted feed) is shown in (Figure 7). This figure represents that increasing the temperature from 543 to 563 K increases the C_{5+} selectivity. However, further increasing

of the temperature to 583K decreases C_{5+} selectivity. Increasing the reactor temperature has two opposite effects: it increases the rate of reactions and on the other hand, it shifts the WGS equilibrium reaction into consumption of CO to produce CO_2. When the reactor inlet temperature increases from 563 to 583K, the second effect is dominant and the production of C_{5+} reduces due to the reduction in the concentration of available CO.

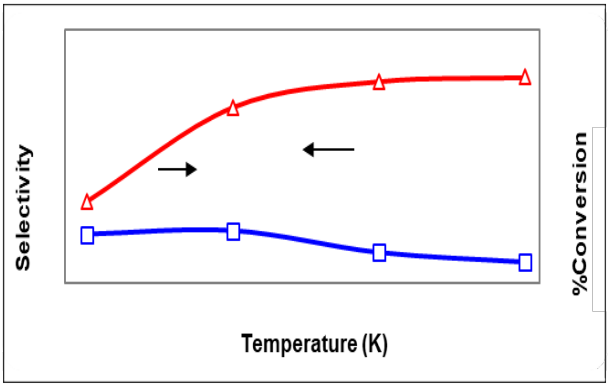

Figure 7. Selectivity of C_{5+} and CO conversion at different temperatures
(P=17 bar, GHSV=5500 hr $^{-1}$ and CO/H_2=1)

(Figure 8) shows that the increase in GHSV, causes a descending trend in the C_{5+} selectivity due to reducing the residence time.

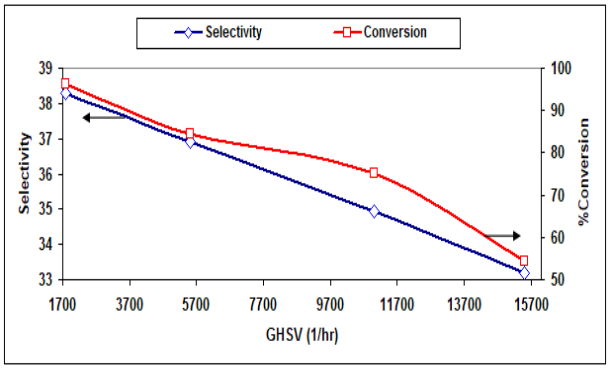

Figure 8. Selectivity of C_{5+} and CO conversion at different GHSVs (T=573, P=17 bar and CO/H_2=1)

The effects of H_2/CO molar ratio on C_{5+} selectivity are presented in (Figure 9). The figure interprets that although increasing the H_2/CO ratio, raises the conversion of CO, but production of heavy hydrocarbons is reduced.

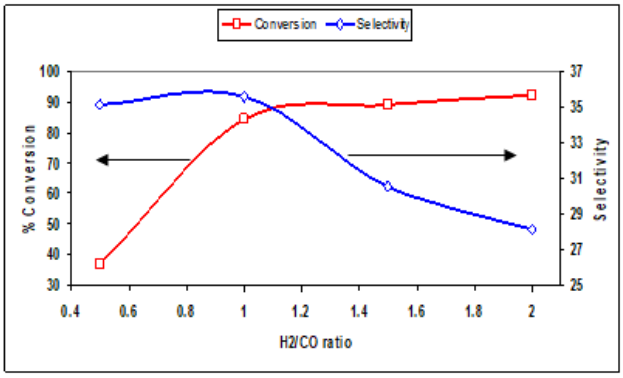

Figure 9. Selectivity of C_{5+} and CO conversion at different H_2/CO molar: (T=573, P=17 bar and GHSV= 5500 hr -1)

The former effect can be related to the fact that hydrogen can participate in termination steps of polymerization reactions [29, 31]. The effect of pressure as another important affecting parameter on this process is investigated in (Figure11). According to this figure, the C_{5+} selectivity increases by increasing total pressure to reach a maximum at a pressure of about 13 bar and thereafter, it takes a descending style. This can be explained by the fact that by increasing the total pressure, the partial pressures of reactants increase which results in increase of C_{5+} and water as products. The presence of water more than a threshold concentration, has a negative effect on C_{5+} selectivity [32].

4. Conclusions

Production of gasoline from Fischer-Tropsch Synthesis (FTS) process in a bench scale fixed-bed reactor was investigated using experiment and CFD modeling. Peng-Robinson equation of state was utilized to model the non-ideality of the gas mixture. The temperature raise at the beginning of catalytic bed was controlled by dilution of catalyst bed with ceramic particles. The simulation results were compared against the experimental data and good agreements were observed. The effects of operating conditions such as temperature, pressure, GHSV and H_2/CO ratio on reactor performance were studied using the validated model. The approximate values of optimum operating conditions were

obtained in order to reach the maximum yield. The optimum values of temperature, pressure, H_2/CO molar ratio were predicted as 563K, 21bar and 1, respectively. The results showed that the C_{5+} selectivity increases by increasing of GHSV. However, economic considerations are needed to obtain the optimum value of GHSV. Since the model has proven to be in good agreement with the experimental data, it could be used in further studies.

Nomenclature

H	Total enthalpy, $kJ.kg^{-1}.s^{-1}$
h	Enthalpy of species, $kJ.kg^{-1}.s^{-1}$
j	Mass flux, $kg.m^{-2}.s^{-1}$
q	Heat flux, $kJ.m^{-2}.s^{-1}$
S	Momentum source term,
D_{ij}	Diffusivity coefficient,
C_i	Concentration, $kmol.m^3$
Z	Compressibility Factor
T	Temperature, K
f	fugacity, bar
k_i	Kinetic Constant, $mol.hr^{-1}.gr^{-1}.bar^{-1}$
E_i	Activation Energy, $kJ.kmol^{-1}$
R	Global Gas Factor, $kJ.kmol^{-1}.K^{-1}$
M_i	Molecular Weight, $kg.kmol^{-1}$
V	Volume, m^3
x_i	Mass Fraction
D	Total Diffusivity Coefficient, $m^2.s^{-1}$
k_m	Thermal Conductivity, $kJ.m^{-1}.K^{-1}$

Greek Letters

ρ	Density, $kg.m^{-3}$
μ	Viscosity, $kg.m^{-1}.s^{-1}$
φi	Fugacity coefficient

Subscript

i	species number
j	second species number
m	mixture

5. References

[1] H. Schulz, Short history and present trends of Fischer-Tropsch synthesis, Appl. Catal. A-Gen.186 (1999) 3-12.

[2] M.E. Dry, The Fischer-Tropsch process: 1950-2000. Catal. Today .71 (2002) 227-241.

[3] J.B. Butt, T. Lin, L.H. Schwartz, Iron alloy Fischer-Tropsch catalysts, VI. FeCo on ZSM-5, J. Catal.97 (1986)261-263.

[4] H. Schulz, H.L. Niederberger, M. Kneip, F. Weil, Synthesis Gas Conversion on Fischer-Tropsch Iron/HZSM5 Composite Catalysts, Stud. Surf. Sci Catal.61 (1991) 313-323.

[5] G. Calleja, A.D. Lucas, R.V. Grieken, Co/HZSM-5 catalyst for syngas conversion: influence of process variables, Fuel.74 (1995) 445-451.

[6] A.P. Steynberg, M.E. Dry, B.H. Havis, B.B. Berman, Chapter 2 Fischer-Tropsch Reactors, Stud. Surf. Sci Catal.152 (2004) 64.

[7] Q.S. Liu, Z.X. Zhang, J.L. Zhou, Steady state and dynamic behavior of fixed bed catalytic reactor for Fischer-Tropsch synthesis. I. mathematical model and numerical method, J. Nat.Gas .Chem, 8 (1999) 137-180.

[8] Q.S. Liu, Z.X. Zhang, , J.L. Zhou, Steady state and dynamic behavior of fixed bed catalytic reactor for Fischer-Tropsch synthesis. II. Steady state and dynamic simulation results, J.Nat.Gas .Chem, 8 (1999) 238-265.

[9] Y. Wang, Y. Xu, Y. Li, Y. Zhao, B. Zhang, Heterogeneous modeling for fixed-bed Fischer-Tropsch synthesis: Reactor model and its applications, Chem. Eng. Sci. 58 (2003) 867-875.

[10] M.R. Rahimpour, S.M. Jokar, Z. Jamshidnejad, A novel slurry bubble column membrane reactor concept forFischer-Tropsch synthesis in GTL technology, Chem. Eng. Res. Des. (2011) In Press.

[11] A. Nakhaei Pour, M.R. Housaindokht, S.F. Tayyari, J. Zarkesh, S.M Kamali Shahri, Water-gas-shift kinetic over nano-structured iron catalyst in FischereTropsch, J. Nat.Gas. Sci. Eng. 2(2010) 79-85.

[12] X.G. Li, D. X. Liuc, S.M Xu, H. Li, CFD simulation of hydrodynamics of valve tray, Chem. Eng. Process. 48 (2009) 145-151.

[13] S. Vashisth, K.D.P. Nigam, Prediction of flow

profiles and interfacial phenomena for

two-phase flow in coiled tubes, Chem. Eng. Process. 48 (2009) 452-463.

[14] A.I. Stamou, Improving the hydraulic efficiency of water process tanks using CFD models, Chem. Eng. Process. 47 (2008) 1179-1189.

[15] M. Rahimi, S.R. Shabanian, A.A. Alsairafi , Experimental and CFD studies on heat transfer and friction factor characteristics of a tube equipped with modified twisted tape inserts , Chem. Eng. Process. 48 (2009) 762-770.

[16] M. Irani, R.B. Bouzarjomehri, M.R. Pishvaei, Impact of thermodynamic non-idealities and mass transfer on multi-phase hydrodynamics, Scientia Iranica 17 (2010) 55-64.

[17] M. Irani, A. Alizadehdakhel, A. Nakhaei Pour, N. Hoseini, M. Adinehnia , CFD modeling of hydrogen production using steam reforming of methane in monolith reactors: Surface or volume-base reaction model? Int. J. Hydrogen. Energy. 36 (2011) 15602-15610.

[18] B. Chalermsinsuwan, P. Kuchonthara, P. Piumsomboon, Effect of circulating fluidized bed reactor riser geometries on chemical reaction rates by using CFD simulations, Chem. Eng. Process. 48 (2009) 165-177.

[19] R. Krishna, J.M. Van Baten, Scaling up bubble column reactors with the aid of CFD, Chem. Eng. Res. Des. 79 (2001) 283-309.

[20] J.M. Van Baten, R. Krishna, Scale Effects on the Hydrodynamics of Bubble Columns Operating in the Heterogeneous Flow Regime, Chem. Eng. Res. Des. 82 (2004) 1043-1053.

[21] C.W. Jiang, Z.W. Zheng, Y.P. Zhu, Z.H. Luo , Design of a two-stage fluidized bed reactor for preparation of diethyl oxalate from carbon monoxide, Chem. Eng. Res. Des. (2011) In press.

[22] G. Arzamendi, P.M. Diéguez, M. Montes , J.A. Odriozola, E.F. Sousa-Aguiar, L.M. Gandía, Computational fluid dynamics study of heat transfer in a microchannel reactor for low-temperature Fischer-Tropsch synthesis, Chem. Eng J. 160 (2010) 915-922.

[23] M. Irani, A. Alizadehdakhel, A. Nakhaeipour, P. Prolx, A.Tavassoli , An investigation on the performance of a FTS fixed-bed reactor using CFD methods, Int. Commun. Heat. Mass. 38 (2011) 1119-1124.

[24] M. Irani, R.B. Bozorgmehry, M.R. Pishvaie, A. Tavasoli , Investigating the Effects of Mass Transfer and Mixture Non-Ideality on Multiphase Flow Hydrodynamics using CFD Methods, Iran. J. Chem. Eng. 29 (2010) 51-60.

[25] A. Nakhaei Pour, M.R. Housaindokht, S. F. Tayyari, J. Zarkesh, Effect of nano-particle size on product distribution and kinetic parameters of Fe/Cu/La catalyst in Fischer-Tropsch synthesis, J. Nat.Gas. Chem. 19 (2010)107-116.

[26] E. A. Foumeny, H. A. Moallemi, C. Mcgreavy, J. A. A. Castro, Elucidation of mean voidage in packed beds, Can. J. Chem. Eng, 69 (2010) 1010-1015.

[27] Fluent, Incorporated: FLUENT 6 USER Manual, Lebanon (NH): Fluent Inc., 2001.

[28] B.E. Poling, J.M. Prausnitz, J.P. O'Connell, The properties of gases & liquids, 5th ed .McGraw-Hill, New York, 2000.

[29] S. Novak, R. J. Madon , and H. Suhl, Secondary effects in the Fischer-Tropsch synthesis, J. Catal. 77 (1982) 141.

[30] B. Sarup and B.W. Wojciechowski, Studies of the Fischer-Tropsch synthesis on a cobalt catalyst i. evaluation of product distribution parameters from experimental data, Can. J. Chem. Eng. 66 (1988) 831.

[31] G.P. Van der Laan, A. A. C. M. Beenackers, Kinetics and Selectivity of the Fischer-Tropsch Synthesis: A Literature Review, Catalysis Reviews, CATAL. REV. SCI. ENG. 41(1999) 255-318.

[32] S. Krishnamoorthy, A. Li, E. Iglesia, Pathways for CO_2 Formation and Conversion During Fischer-Tropsch Synthesis on Iron-Based Catalysts, Catal. Lett. 80 (2002) 77-86.

افزایش راندمان تولید سوخت مایع با استفاده از کاتالیست نانو آهن در فرآیند تبدیل گازطبیعی به مایع

- محمد ایرانی[1*] ،اصغر علیزاده داخل[2]، یحیی زمانی[1]

۱. پژوهشگاه صنعت نفت، تهران، ایران

۲. گروه شیمی و مهندسی شیمی، واحد رشت، دانشگاه آزاد اسلامی، رشت، ایران

(ایمیل نویسنده مسئول: iranim@ripi.ir)

چکیـــــــده

در این مقاله یک بررسی تجربی و مطالعه CFD با هدف افزایش تولید بنزین با استفاده از فرآیند فیشر- تروپش در یک رآکتور در مقیاس رومیزی (بنچ) انجام گرفت. یک رآکتور استوانه ای با یک منطقه پیش گرم کن و یک منطقه واکنش بکار گرفته شد. دمای رآکتور با استفاده از یک گرمکن کمربندی دور رآکتور، کنترل گردید. همچنین یک مدل CFD با تقارن ودر نظرگرفتن غیر ایده آلی مخلوط گازی با استفاده از معادله حالت پنگ - رابینسون ، توسعه داده شد. تعداد واکنشهای به کار گرفته شده برای این مدل ۲۳ مورد بود. مدل توسعه داده شده با اطلاعات تجربی اعتبارسنجی گردید. مدل تایید شده برای بررسی اثر شرایط عملیاتی روی کارکرد رآکتور استفاده شد. مقادیر بهینه شرایط عملیاتی شامل فشار ، دما، GHSV ونسبت خوراک برای کارکرد بهینه رآکتور بدست آمدند.

واژگان کلیدی: سنتز فیشر-تروپش، جی تی ال، رآکتور بستر ثابت، کاتالیست نانو آهن، سی اف دی